Reduced H3K27me3 suppresses Wnt/β-catenin signaling by S-adenosylmethionine deficiency in neural tube development

Li Zhang
Shanxi Medical University
Xiuwei Wang
Capital Institute of Pediatrics
Dandan Li
Shanxi Medical University
Yufei Wang
Shanxi Medical University
Xueqin Liu
Shanxi Medical University
Rui Cao
Biology Institute of Shanxi
Keke Wang
Shanxi Medical University
Zhizhen Liu
Shanxi Medical University
Bo Niu (niub2004@126.com)
Shanxi Medical University https://orcid.org/0000-0001-5486-6211
Jun Xu
First Hospital of Shanxi Medical University
Jun Xie
Shanxi Medical University

Research Article

Keywords: Neural tube defects, S-adenosylmethionine, Wnt/β-catenin signaling, H3K27me3, differentiation

Posted Date: November 2nd, 2021

DOI: https://doi.org/10.21203/rs.3.rs-562510/v2

Abstract

S-adenosylmethionine (SAM) as a major methyl donor play a key role in methylation modification *in vivo*, and its disorder was closely related to neural tube defects (NTDs). However, the underlying mechanism between SAM deficiency and NTDs remained unclear. Here, we investigated the association between histone methylation modification and Wnt/β-catenin signaling pathway in NTDs induced by SAM deficiency. The levels of SAM and SAH were determined by enzyme linked immunosorbent assay (ELISA). The expressions of H3K27me3 and Wnt/β-catenin signaling pathway specific markers were demonstrated by western blotting, reverse transcription, and quantitative PCR (RT-qPCR) and immunofluorescence in ethionine induced E11.5 mouse NTDs and NSCs models. The results showed that the incidence rate of NTDs induced by ethionine were 46.2%, post treatment of ethionine combined with SAM, the incidence rate of NTDs was reduced to 26.2%. The level of SAM was significantly decreased (P<0.05) and a reduction in the SAM/SAH ratio was observed. The SAM depletion caused the reduction of both H3K27me3 modifications and UTX activity, and inhibited the marker proteins (β-catenin, TCF-4, Axin-2, p-GSK-3β, CyclinD1, and C-myc) in Wnt/β-catenin signaling pathway (P<0.05). The differentiations of neural stem cells (NSCs) into neurons and oligodendrocytes were inhibited under SAM deficiency (P<0.05). These results indicated that the depletion of SAM led to reduced H3K27me3 modifications, prevented the activation of Wnt/β-catenin signaling pathway and NSCs differentiation, which provided an understanding of the novel function of epigenetic regulation in NTDs.

Introduction

Abnormal development of central nervous system (CNS) caused by neural tube defects (NTDs), including anencephaly, spina bifda, and encephalocele et al, not only remained a major contributor in the prevalence of stillbirths and neonatal deaths, but also a significant cause of lifelong physical disability in the surviving infants. Human NTDs was considered to be associated with genetic and environmental factors [1]. The genetic predisposition is not yet well understood, but environmental factors such as maternal folic acid have been identified as closely related to NTDs. It had been established that maternal folate supplementation decreased/prevented the occurrence of NTDs [2], and folate fortification was mandated in some other countries. However, the underline molecular mechanisms between folate deficiency and NTDs remained unclear.

Folate metabolism is essential nutrients required for the two major biological processes, including purine and thymidine monophosphate biosynthesis and methionine regeneration. S-adenosylmethionine (SAM), a key metabolite in the methionine regeneration, acts as a major methyl donor in numerous biochemical reactions [3, 4]. It has reported that that abnormalities of SAM were associated with NTDs [5]. Ethionine is biologically antagonistic to methionine, which is an S-ethyl homologue of methionine [6, 7]. It competed with methionine and thus resulted in reduction of SAM during DNA, RNA and proteins synthesis [8]. Furthermore, previous studies have confirmed that ethionine could cause NTDs in the whole embryo culture [5, 8]. However, the pathogenesis of methionine circulation in NTDs was not clearly clarified. Thus, it is crucial to explore the molecular mechanisms of SAM involved both in prevention of NTDs and its potential role in human brain development.

Experimental studies indicate that β-catenin was the primary effector molecule in the Wnt/β-catenin signaling pathway [9], and playing a major role in cell growth and survival [10]. In addition, Wnt/β-catenin signaling had a major role in maintaining self-renewal as well as in regulating NSCs differentiation [11]. Increasing evidence implicated that the SAM was closely related to the Wnt/β-catenin signaling. It was reported that SAM treatment reduced the expression level of total β-catenin, in dedifferentiated cells [12]. Moreover, β-catenin signaling was regulated by SAM level in hepatocytes [13]. β-catenin signaling was required for caudal neural tube closure, and closely related to the occurrence of NTDs. However, it has not reported that whether the depleted of SAM affected the histone methylation, activated Wnt/β-catenin signaling pathway, and inhibited the differentiation of NSCs into neurons and oligodendrocytes, finally resulted in the occurrence of NTDs. Here, our studies showed that SAM activated Wnt/β-catenin signaling pathway by increasing histone methylation

and strengthening cell differentiation. This study not only contribute to a better understanding of the molecular mechanisms responsible for the regulation of SAM but also provide new therapeutic targets for the treatment of NTDs.

Materials And Methods

Animals

C57BL/6 mice (9-10 week, weighing 19-23 g), were provided by Shanxi Medical University which were housed in specific pathogen-free cage with an approve facilities following a 12 hours light/dark cycle. Mature male and female C57BL/6 mice were allowed to mate overnight and vaginal plug was observed in the following morning. Noon of the day on which vaginal plug was detected, was considered as embryonic day 0.5 (E0.5). On E7.5, mice were randomly divided into two groups: control group and NTD mice model (established by intra-peritoneal injection of ethionine). The pregnant mice were sacrificed by cervical dislocation on E11.5. All embryos were dissected under a stereoscopic microscope, and the phenotype was recorded. Some embryos were fixed in cold 10% neutral buffered formalin for subsequent hematoxylin and eosin staining. All procedures involving animal handling were approved by the Animal Research Ethics Board of Shanxi Medical University, China.

Cell culture and treatment

Primary neural stem cells (NSCs) were isolated from mice embryos on E13.5. Briefly, the brain vesicle of mouse embryo was collected under sterile conditions, suspended as single cell in 5 mL DMEM/F12 medium (Hyclone, Logan, UT, USA) supplemented with 2% B27 (Gibco, USA), EGF (20 ng/mL, Peprotech, USA), and b-FGF (20 ng/mL, Peprotech, USA). The cells were incubated at 37°C with 5% CO_2 and passaged after every 3 days. NSCs were passaged at least twice before they were used for the subsequent experiments. The cells were treated with 20 mmol/L ethionine, 2mmol/l SAM for 48 hours, and 30 nmol/l of UTX inhibitor GSK J4 sc-391114 (Santa Cruz, USA) for 6 hours.

Hematoxylin-eosin staining

The E11.5 embryos paraffin sections were deparaffinized with xylene, soaked in 100, 95, 80 and 75% ethanol for 3 minutes each. After washing with distilled water for 2 minutes, hematoxylin stain was performed for 5 minutes, and washed with tap water. Hydrochloric acid and ethanol were applied for 30 seconds, washed again 5 times under running tap water and finally soaked in tap water for 15 minutes. Post keeping in eosin solution for 2 minutes, normal dehydration, clearing and neutral resin sealing were carried out.

Western blot analysis

Proteins were extracted from E11.5 embryo brain tissues and NSCs. Total protein concentration was determined using a BCA protein assay kit (Pierce/Thermo Fisher, USA). The proteins were denatured in SDS gel-loading buffer at 95℃ for 8 minutes, 30 μg of each sample was separated on 12% SDS-PAGE gel and then transferred onto polyvinylidene fluoride (PVDF) membranes (Millipore, Billerica, MA, USA). After blocking with 5% skim milk at room temperature for 1 h, the membrane was incubated with primary antibodies overnight at 4℃ followed by incubation with the secondary antibody at room temperature for 2 hours. The protein bands were visualized using an enhanced chemiluminescent (ECL) blot detection system (ChemiDoc™ Imaging Systems, BIO-RAD, USA) following manufacture's instruction. The protein bands were quantified using ImageJ software, and β-Tubulin, β-actin, and GAPDH were used as a control.

Enzyme linked immunosorbent assay (ELISA)

On E11.5, mice were anesthetized with chloral hydrate and blood was collected from the eyeball. Serum was separated and the concentration of SAM and SAH were evaluated using the SAM and SAH ELISA kit (R&D Systems; Minnesota, USA) according to the manufacturer's protocol.

Total RNA extraction, reverse transcription, and quantitative PCR (RT-qPCR)

Total RNA was extracted using trizol method (Invitrogen, Carlsbad), and cDNA was synthesized using Revert Aid First Strand cDNA Synthesis Kit (Thermo, USA). Maxima SYBR Green/ROX qPCR Master Mix (Takara, Japan) were used for qPCR. The data was analyzed with $2^{-\triangle\triangle}$Ct method and the mRNA level was normalized with β-actin (B661302-0001, Sangon, Shanghai). Primer sequences were shown in table 1.

Table 1. Primer Sequences Used for RT-PCR Analysis

Symbol	Forward Primer (5'-3')	Reverse Primer (5'-3')
EZH2	AGTTCGTGCCCTTGTGTGATAGC	ACTCTCGGACAGCCAGGTAGC
Kdm6a	TGCCTCTGCCTTCACCTCTACC	CGCCTCCAATCTCCGCACAAG
Kdm6b	GGCTCTTTGATTTCCCACCCACTC	TGCTGCTGCTCCTCCTCCTTC
β-catenin	TGCAGTTCGCCTTCACTAGA	ACTAGTCGTGGAATGGCACC
Axin-2	TGGAGAACTCAAATCTTCGACA	ATCTGTCCAGAAGAAGCCATAG
GSK-3β	AGGAGAACCCAATGTTTCGTAT	ATCCCCTGGAAATATTGGTTGT
C-myc	AAATCCTGTACCTCGTCCGATT	CCACAGACACCACATCAATTTC
CyclinD1	CGTATCTTACTTCAAGTGCGTG	ATGGTCTCCTTCATCTTAGAGG

Immunofluorescence

NSCs were resuspended and adjusted to a density of 1×10^5 cells/mL and seeded (1 mL) into each well of the 24-well plate chamber slides pre-coated with poly-lysine (Solabio, China). 20 mmol/l ethionine and 2 mmol/l SAM treatment for 24h, the cells were washed 3 times with cold PBS. NSCs were fixed in 4% paraformaldehyde for 10 minutes at room temperature and washed again 3 times with PBS. After treatment with 0.3% Triton X-100 and blocking with 5% BSA for 1h, NSCs were incubated with diluted antibody with biotin overnight at 4℃. After washing with PBS, the cells were incubated with secondary antibodies for 1 hour at room temperature, washed with PBS again and stained with DAPI (Sigma-Aldrich, St. Louis, MO) for 10 min at room temperature. Images were captured with the help of a fluorescence microscope (Nikon, Tokyo, Japan). The antibodies used for immunofluorescence staining were: the mouse monoclonal anti-Nestin antibody (1:500, Abcam, UK) for neural precursor cells, rabbit monoclonal anti-microtubule-associated protein 2 (Map2; 1:500; Abcam, UK) for neurons, mouse monoclonal anti-glial fibrillary acidic protein antibody (GFAP, 1:500, Abcam, UK) for astrocytes, rabbit monoclonal Galactosylceramidase (GLAC, 1:500; Abcam, UK) for oligodendrocytes, rabbit monoclonal neurofilament antibody (NF-H, 1:500, Abcam, UK) for neurons, rabbit monoclonal anti-H3K27me3 antibody (1:500, Abcam, UK), β-catenin (1:500, Abcam, UK), Cyclin D1 (1:100, Abcam, ab16663) and Axin-2 (1:50, Santa Cruz Biotechnology).

For immunohistochemical staining, paraffin sections (5-mm thick) were subjected to high temperature antigen retrieval for 5 minutes in microwave oven in 1mM Tris-EDTA buffer (pH 9.0). Slides were treated in 3% H_2O_2 for 20 minutes and blocked in 5% normal goat serum in PBS with 10% avidin for 1 hour. Block solution was washed by PBS, and the slides were incubated with diluted antibody in biotin overnight at 4℃. After washing with PBS, the slides were incubated again with secondary antibodies for 1 hour at room temperature, washed with PBS, and then stained with DAPI for 10 minutes at room temperature. Images were captured using a fluorescence microscope (Nikon, Tokyo, Japan). The antibodies used for immunofluorescence staining were H3K27me3 (1:500, Abcam, UK), β-catenin (1:500, Abcam, UK), Cyclin D1 (1:100, Abcam,

ab16663), TCF-4 (1:50, Santa Cruz Biotechnology, sc-166699) and P53 (1:200, Abcam, ab131442) in E10.5 and E11.5 embryos.

UTX activity detection

UTX activity was detected according to the manufacturer's protocol using apparent enzyme JMJD3/UTX demethylase Activity/Inhibition Assay Kit (Epigentek, Farmingdale, NY). 10μg nuclear extract was used for detection.

Functional Interact Network Analysis of DEGs

The key DEG in the development of the mouse neural tube is Screening is performed by using an intersection analysis between control and ethionine. The expression patterns of the selected DEGs were analyzed by clustering 3.0 [14] and Java Treeview [15].

Statistical Analysis

Statistical analysis was performed using GraphPad Prism version 6.0 (GraphPad

Software, CA) and the data was presented as mean ± SEM. The *t*-test was used for the the comparisons of two groups, while for multiple comparison test, ANOVA followed by Tukey post hoc test were performed. *P* values<0.05 were considered as statistically significant.

Results

Ethionine induces neural tube defects by disrupting methionine cycle

Methionine is an important morphogen for the normal development of brain. In previous study, we had demonstrated that 500 mg/kg of ethionine caused the highest incidence rate (54.8%) of NTDs with a lower embryonic resorption rate (8.2%) [16]. Therefore, this dose of ethionine (500mg/kg) was used to establish the NTDs mouse model. The results showed that a full appearance of the structural characteristics was observed in the control embryos (Figure 1A). Compared with E11.5 control mouse embryos, 500 mg/kg ethionine treated embryos showed an obvious overall growth retardation along with a small and hypoplastic brain vesicle (figures 1B-D). Compared with the control, NTDs revealed that neural tube closure was failed in the hindbrain region (Figures 1E-F).

In order to investigate whether ethionine induced NTDs by disrupting the methionine cycle. SAM were intraperitoneally injected into the NTDs model on E7.5 to observe the incidence of NTDs. The results showed that the incidence rate of NTDs induced by ethionine were 46.2%. Post treatment of ethionine combined with SAM, the incidence rate of NTDs was reduced to 26.2% as shown in Table 1. However, it was found that ethionine at 500 mg/kg and SAM at 30 mg/kg dose had no effect on the weight gains during pregnancy (Table 3, Figures 1G-I). The level of SAM was significantly decreased in 500mg/kg ethionine treated group compared with the control group in mouse embryonic tissue (Figure 1J). Compared with the control group, SAH level was significantly decreased in NTDs mouse embryonic tissue (Figure 1K), and a consequent reduction in the SAM/SAH ratio was observed (Figure 1L). These findings indicated that ethionine induced NTDs via blocking the generation of SAM.

Table 2
Embryonic phenotypes of mice treated with ethionine and SAM.

	Pregnant mice (n)	Embryos (n)	Normal n (%)	Resorption n (%)	Growth retardation n (%)	NTDs n (%)	Other malformation n (%)
SAM	38	248	229(92.2)	6(2.4)	13(5.2)	0(0)	0(0)
Ethionine	31	199	44(22.1)	19(9.5)	29(14.6)	92(46.2)	11[a]4[b] (15.1)
Ethionine+SAM	33	214	128(59.9)	11(5.1)	14(6.5)	56(26.2)	3[a]2[b] (2.3)

[a] craniofacial malformation[b] polydactyly

Table 3
The effects of 500 mg/kg Ethionine and 30 mg/kg SAM treatment on pregnant mice.

Ethionine (mg/kg)	SAM (mg/kg)	No. injected	No. dead	E7.5 body weight (g)	E11.5 body weight (g)	E11.5 body gain[a] (g)	Untoward reaction
0	0	11	0	21.33 ± 0.4613	27.91 ± 0.2417	6.580 ± 0.4307	0
0	30	11	0	20.77 ± 0.321	28.09 ± 0.306	7.318 ± 0.354	0
500	0	11	0	20.69 ± 0.3362	28.38 ± 0.2508	7.697 ± 0.4473	0
500	30	11	0	20.942 ± 0.267	27.96 ± 0.228	7.020 ± 0.377	0

[a] Weight gain refers to the body weight of E11.5 compared with E7.5.

SAM enhances the histone methylation level of E11.5 embryonic brain tissue and NSCs

SAM, as a methyl donor, affects histone methylation modification. To investigate whether the depleted of SAM could affected the methylation of histones in NTDs. The levels of histone methylation were determined in E11.5 embryonic brain tissue and NSCs. The results showed that the expression of H3K4me3, H3K27me3, H3K36me3 and H3K79me3 in E11.5 ethionine-induced embryonic brain tissues were significantly decreased compared with normal embryonic brain tissue, especially H3K27me3 expression (Figure 2A). Meanwhile, high expression level of H3K27me3 was observed in normal embryos, which was lowered in NTDs embryos. Consistent with the abovementioned results, H3K27me3 was significantly down-regulated in NTDs embryos (Figure 2B). In contrary, the expression of H3K27me3 was markedly increased in ethionine and SAM-treated group compared with the ethionine-treated group (Figure 2B). H3K27me3 possessed specific methylation modification enzymes, including methyltransferase Ezh2, demethylase UTX and JMJD3, which are encoded by *Ezh2*, *Kdm6a* and *Kdm6b* genes, respectively. Here, the expression of *Ezh2*, *Kdm6a* and *Kdm6b* were detected to investigate the association between those enzymes and H3K27me3. The results demonstrated that the expression of *Ezh2* mRNA was significantly decreased in ethionine group compared with control. Simultaneously, ethionine also increased the expression of *Kdm6a* and *Kdm6b* which negatively regulated the expression of H3K27me3 (Figure 2C). Conversely, the situation was reversed after SAM supplementation. Thus, it was concluded that SAM improved histone methylation levels by increasing methyl donors.

To further prove the role of SAM in histone methylation, we have determined the histone methylation levels in neural stem cells. The neural stem cells (NSCs) were obtained from E13.5 mouse embryos, which were major cell types in CNS development [17]. The morphology of NSCs isolated from the mouse embryos was normal and globular in appearance (Figures 3A-D). It was strongly expression of Nestin, neural stem cell marker, in the isolated NSCs (Figures 3I-K), and the NSCs could differentiate into Map2-positive neurons, GLAC-positive, NF-H-positive and GFAP-positive astrocytes (Figures 3E-H).

The histone methylation expression was determined in the NSCs treated with 20mmol/L ethionine and 2mmol/l SAM. The results showed that the expression levels of H3K4me3, H3K27me3, H3K36me3 and H3K79me3 were significantly decreased in ethionine group compared with the normal group. Compared with ethionine group, the expression levels and H3K27me3-positive cell numbers were robustly up-regulated in ethionine+SAM treated group (Figures 3L and 3M). In addition, a significant decrease was observed in *Ezh2* level in ethionine group compared with the control group, and the expression of *Kdm6a* and *Kdm6b* were increased significantly in the ethionine-treated group compared with cells in the control group. The expression of *Ezh2, Kdm6a* and *Kdm6b* were negatively regulated the expression of H3K27me3. Similarly, SAM supplementation could partially reverse this phenomenon (Figure 3N).

Sam Regulates Cell Function Via Activating Wnt/β-catenin Signaling

Wnt/β-catenin signaling pathway involved in embryonic neural development and neural tube closure, especially NTDs [18, 19]. In our previous study, we have demonstrated the depleted SAM could lead to the occurrence of NTDs. Then, in order to investigate whether the depleted SAM inactivated the Wnt/β-catenin signaling pathway in embryonic development, finally result in the occurrence of NTDs, the relative expression of several protein markers related to Wnt/β-catenin signaling pathway (β-catenin, TCF-4, Axin-2, p-GSK-3β, CyclinD1, and C-myc) was determined in embryos and NSCs. The results showed that the proteins related to the Wnt/β-catenin pathway (β-catenin, TCF-4, Axin-2, p-GSK-3β, CyclinD1, and C-myc) were inhibited in ethionine treated group compared with the control (Figure 4A). It was found that the expression levels of β-catenin, TCF-4, Axin-2, p-GSK-3β, CyclinD1, and C-myc were upregulated in ethionine+SAM group compared with the ethionine group (Figures 4A-B). Compared to the control group, an obvious decrease in the proportion of β-catenin$^+$, TCF-4$^+$, CyclinD1$^+$ cells relative to that of DAPI$^+$ cells were observed in ethionine-treated group (Figure 4C). Meanwhile, SAM supplementation reversed this situation in embryos.

In order to further investigate whether the decreased level of SAM caused the inactivation of Wnt/β-catenin pathway, the protein expression level of β-catenin, TCF-4, Axin-2, p-GSK-3β, CyclinD1, and C-myc in NSCs treated with 20mM ethionine and 2mM SAM for 48h were measured. The results showed that there were significant decreased levels of CyclinD1, Axin-2, C-myc, β-catenin and TCF-4 in ethionine treated group (Figure 5A-B). GSK-3β plays a key role in the canonical Wnt pathway which operates through regulating the phosphorylation and degradation of the transcription activator β-catenin. The effect of ethionine on GSK-3β showed that p-GSK-3β and GSK-3β were down-regulated in ethionine treated group compared with control, and p-GSK-3β and GSK-3β were up-regulated in ethionine+SAM group compared with ethionine group (Figure 5C). Furthermore, compare to control group, significant decreased expression of CyclinD1, Axin-2 and β-catenin were observed in NSCs with 20mM ethionine (Figure 5D).

Reduced Utx Activates Wnt/β-catenin Signaling Pathway

Recent studies reported that UTX, a key factor for neural tube development, was H3K27me3 demethylase. In order to ensure the decreased level of H3K27me3 caused by UTX inactivated Wnt/β-catenin signaling pathway in ethionine-induced NSCs, the UTX function was determined. Results showed that UTX activity was significantly down-regulated after the treatment of ethionine (Figure 6A), and ethionine treatment suppressed the expression of *β-catenin*, *CyclinD1*, *C-myc*, and

*GSK-3β (*Figures 7C-F) and increased the expression level of *Axin-2* (Figure 6B) which negatively regulates the process of Wnt/β-catenin signaling pathway. On contrary, the UTX demethylase inhibitor-GSK-4J activated Wnt/β-catenin signaling pathway, by up-regulating the expression level of *β-catenin*, *CyclinD1*, *C-myc*, and *GSK-3β* and down-regulating the expression of *Axin-2* (Figures 6B-F). Furthermore, the expression levels of *β-catenin*, *CyclinD1*, *C-myc*, and *GSK-3β* genes were significantly up-regulated with ethionine combined with GSK-4J treatment, while slightly down-regulated *Axin-2* (Figures 6B-F).

SAM enhances NSCs differentiate into neurons and astrocytes

It was investigated whether the role of SAM deficiency could inhibit terminal mitosis of NSCs and hinder neuronal differentiation. As exhibited in the schematic diagram, the expressions of anti-MAP2, anti-GFAP, anti-GLAC and anti-NF-H were detected in control, ethionine-treated, SAM-treated and ethionine+SAM-treated NSCs groups. The results showed an obvious decreased in the proportions of $MAP2^+$, $GFAP^+$, $GLAC^+$, $NF\text{-}H^+$ cells relative to the DAPI+ cells were observed in the ethionine-treated group compared with the control one (Figure 7A). To investigate the dynamic changes of gene expression during neural tube development, the gene expression level of two embryo samples was compared for each other. In Control-vs-Ethionine comparison, DEGs were significantly enriched in secondary active transmembrane transporter activity, adrenal chromaffin cell differentiation, hemoglobin complex, transmembrane transporter activity, neuroendocrine cell differentiation, noradrenergic neuron development, oligodendrocyte development (Figure 7B). These results indicated that ethionine inhibited NSCs terminal mitosis and thus reduced neural differentiation.

Discussion

In this study, we reported that the depleted of SAM was involved in the pathogenesis of NTDs. Furthermore, experiments using a mouse model of maternal SAM depletion revealed that intracellular SAM depletion led to an impairment of histone methylation that was associated with activation of the Wnt/β-catenin pathway. Additionally, further analyses suggested that SAM deficiency could inhibit terminal mitosis of NSCs and hinder neuronal differentiation. Taken together, our findings raise the possibility that SAM involved in the development of NTDs through inhibition of histone methylation and activation of Wnt/β-catenin signaling pathway which affected the NSCs differentiation.

The neural tube closure process relies on the synergy of multiple mechanisms, including the convergence and extension of neural plate, migration of nerve cells, proliferation and apoptosis of neuroepithelial cells, and contraction of the cytoskeleton filaments of the root tip. Studies have shown that the interaction of genetic and environmental factors contributed to the neural tube closure [1, 20, 21]. Any destruction in the process of neural tube closure could lead to the occurrence of NTDs. Until now, the pathogenesis of NTDs and the effective mechanism of folate in preventing of NTDs remain unclear. Previous studies suggested that epigenetic modifications including DNA methylation and histone methylation played a key role in the occurrence of NTDs [22, 23]. It was speculated that the folate deficiency might lead to the decreased of SAM, as a major methyl donor, which caused the abnormal methylation modification *in vivo*, and then resulted in the occurrence of NTDs. In order to verify this hypothesis, we established the NTDs mouse model via injecting the ethionine and inhibiting the synthesis of SAM [16]. Here, we had simultaneously given ethionine along with SAM to the pregnant mice. The results showed that the incidence of NTDs was significantly decreased, and the levels of SAM and SAM/SAH ratio were significantly higher in ethionine+SAM group compared with ethionine group. It was further confirmed that the NTDs mouse model were induced by SAM metabolic disorder. These results suggested that SAM played crucial role in neural tube development.

The epigenetic modification in the neural tube development had received increased attention in recent research, and specific histone methylation spatiotemporal expression patterns might be essential for neurogenesis. Histone methylation played important roles in implicating chromatin modification and gene activation or repression, which depended on the methylation of site-specific residue. Studies had reported that there were 24 histone methylation sites, including 17 on

lysine residues and 7 on the arginine residues, in which H3K4me3, H3K36me3 and H3K79me3 were related to gene activation, and H3K9me3 and H3K27me3 were related to gene silencing [24–26]. The regulation of histone methylation modification were widely involved in neural tube development [27, 28]. The modification level of H3K9me3 and H4K20me3 were significantly reduced after feeding with methyl deficient food in rats [29]. Previous studies also showed that histone methylation modification could directly or indirectly activate and inhibit gene expression, thereby affecting embryonic development [30]. It was revealed that valproic acid caused the increased of H3K4me3, and decreased of H3K9me3 in the NTDs mouse model, respectively [31]. In our study, the results showed that histone methylation modification was significantly decreased in ethionine-induced NTDs embryos, which were consistent with the alteration of H3K79me3 and H3K27me3 in human NTDs samples [27, 32]. Moreover, we also found that the SAM metabolism disorders caused the alteration of histone methylation modifications in NSCs, and the alteration could be improved by SAM supplementation. It was suggested that SAM metabolic disorder could affect the histone methylation modification, finally caused the occurrence of NTDs.

It was well known that Wnt/β-catenin signaling pathway was essential for neural development [33]. Some studies showed that β-catenin, a key transcriptional regulator, was closely relate with NTDs occurrence [34]. It was reported that SAM treatment reduced the expression level of total β-catenin, in dedifferentiated cells [23]. Moreover, β-catenin signaling was regulated by SAM level in hepatocytes [35]. Based on this, we speculated that the depleted of SAM affected the Wnt/β-catenin signaling pathway, and resulted in NTDs. In our study, the results showed that the expression of β-catenin, TCF-4 and CyclinD1 was significantly reduced in the ethionine group, and reversed by SAM supplementation. These results suggested that SAM deficiency inhibited Wnt/β-catenin signaling pathway. As above, SAM deficiency caused an abnormal histone methylation modification. Therefore, we speculated that SAM deficiency induced abnormal expression of histone methylation modification, inhibited the activation of Wnt/β-catenin signaling pathway, and thus participated in the occurrence of NTDs. Here, our results showed that UTX, a H3K27me3 demethylase, activity and the expression of β-catenin, CyclinD1, C-myc, and GSK-3β were significantly decreased, the expression of Axin-2 were significantly increased after the treatment of ethionine. On contrary, the UTX demethylase inhibitor-GSK-4J activated Wnt/β-catenin signaling pathway, by up-regulating the expression level of β-catenin, CyclinD1, C-myc, and GSK-3β and down-regulating the expression of Axin-2. The results indicated that SAM deficiency induced abnormal expression of H3K27me3, and inhibited the activation of Wnt/β-catenin signaling pathway. However, these findings were not in agreement with the reports that SAM could inhibit β-catenin signaling in dedifferentiated cells [36, 37]. Lastly, we evaluated the expression and activity of H3K27me3 in ethionine-treated NSCs. UTX, also known as Kdm6b, belongs to a small family of JmjC-domain containing enzymes that mediate demethylation of H3K27me3 repressive chromatin marks [38]. Our study showed that ethionine caused an increased UTX activity, which lead to increased H3K27me3 expression level. RT-qPCR results suggested that reduced UTX activate Wnt/β-catenin signaling pathway by increasing the level of H3K27me3. In short, we inferred that this inconsistency was due to SAM-SAH metabolic disorder and these abnormal metabolites were caused by ethionine. It was implied another possibility that SAM might stimulate Wnt/β-catenin signaling pathway through activation of histone methylation.

Wnt/β-catenin signaling had a major role in maintaining self-renewal as well as in regulating NSCs differentiation [39]. In order to investigate the association between the Wnt/β-catenin signaling pathway and the NSCs differentiation, we choose the primary neural stem cells extracted from E13.5 embryos as a cell model treated with ethionine. The results demonstrated that SAM depletion prevented NSCs differentiate into neurons and oligodendrocytes and inhibited Wnt/β-catenin signaling pathway activation. Furthermore, ethionine impaired NSCs differentiation which was partially rescued by SAM supplementation. These results reinforced the idea that SAM positively regulated NSCs differentiation. Similar notion was raised in a previous research revealing that SAM metabolism level was related to cell differentiation [23].

Conclusions

Collectively, our results uncovered the essential role of SAM in modulating Wnt/β-catenin signaling pathway during neurogenesis and normal neurodevelopment. SAM reduction disturbed NSCs differentiation and resulted in developmental disorders. Our research also revealed that the depletion of SAM led to reduced H3K27me3 modifications and UTX activity downregulation, prevented the activation of Wnt/β-catenin signaling pathway and accelerated NSCs differentiation. These results provided a new understanding of the novel function of epigenetic regulation in NTDs which will have far-reaching implications in diseases and neurobiology. Hence, the mechanisms and influences of these altered epigenetic histone modifications needs to concrete studies in future.

Declarations

Author contributions

LZ and XW wrote the manuscript. AK and FW helped in revising the manuscript. LZ, DL and ZL analyzed the data. KW contributed to the manuscript for literature research. JX, JX and BN revised and approved the manuscript. All authors read and approved the manuscript for submission.

Ethics approval and consent to participate

Not applicable.

Consent for publication

Not applicable.

Competing interests

The authors declare that they have no competing interests.

Acknowledgements

We thank all the mice which contributed to this study.

Availability of data and materials

All the data generated or analyzed during this study are included in this article.

Funding

This study was supported by grants from the National Natural Science Foundation of China (No. 81671462), the Beijing Municipal Natural Science Foundation (No.7182025), Natural Science Foundation of Shanxi Province (20210302124291), Natural Science Foundation of Health Commission of Shanxi Provincial (2020090), and School-level Doctoral Foundation of Shanxi Medical University (XD2005SD2004).

References

1. Wallingford, J. B., Niswander, L. A., Shaw, G. M., & Finnell, R. H. (2013). *The continuing challenge of understanding, preventing, and treating neural tube defects* (339 vol., pp. 1222002). New York, NY: Science
2. Prevention of neural tube defects: results of the Medical Research Council Vitamin Study. MRC Vitamin Study Research Group. (1991). *Lancet (London, England)*, 338, 131–137
3. Caboche, M. (1976). Methionine metabolism in BHK cells: selection and characterization of ethionine resistant clones. *J Cell Physiol*, 87, 321–335

4. Van Winkle, L. (2019). Ryznar RJFic, biology d. One-Carbon Metabolism Regulates Embryonic Stem Cell Fate Through Epigenetic DNA and Histone Modifications: Implications for Transgenerational Metabolic Disorders in Adults. *Frontiers in cell developmental biology*, 7, 300
5. Leung, K. Y., Pai, Y. J., Chen, Q., Santos, C., Calvani, E., Sudiwala, S. … Greene, N. D. E. (2017). Partitioning of One-Carbon Units in Folate and Methionine Metabolism Is Essential for Neural Tube Closure. *Cell reports*, 21, 1795–1808
6. PATTERSON, E. L., HASH, JH, LINCKS, M., MILLER, PA, BOHONOS, N. E. T. H. Y. L. A. T. I. O. N., & Science BIOLOGICAL FORMATION. (1964). (New York, NY) 146:1691–1692
7. Alix, J. H. (1982). Molecular aspects of the in vivo and in vitro effects of ethionine, an analog of methionine. *Microbiological reviews*, 46, 281–295
8. Dunlevy, L. P., Burren, K. A., Mills, K., Chitty, L. S., Copp, A. J., & Greene, N. D. (2006). Integrity of the methylation cycle is essential for mammalian neural tube closure. Birth defects research. Part A, Clinical molecular teratology. 76:544–552
9. Anastas, J. N., & Moon, R. T. (2013). WNT signalling pathways as therapeutic targets in cancer. *Nature reviews. Cancer*, 13, 11–26
10. Klaus, A., & Birchmeier, W. (2008). Wnt signalling and its impact on development and cancer. *Nature reviews Cancer*, 8, 387–398
11. Chen, C., Yang, Y., & Yao, Y. (2019). HBO Promotes the Differentiation of Neural Stem Cells via Interactions Between the Wnt3/β-Catenin and BMP2 Signaling Pathways. *Cell transplantation*, 28(12), 1686–1699
12. Liu, Y., Lv, W., Yu, B., Ju, T., Yang, F., Jiang, M. … Huang, J. (2013). S-adenosylmethionine-induced adipogenesis is accompanied by suppression of Wnt/β-catenin and Hedgehog signaling pathways. *Molecular and cellular biochemistry*, 382, 59–73
13. Li, T., Peng, H., Yang, H., Kurniawidjaja, S., Panthaki, P., Zheng, Y. … Lu, S. (2015). S-Adenosylmethionine and methylthioadenosine inhibit β-catenin signaling by multiple mechanisms in liver and colon cancer. *Molecular pharmacology*, 87, 77–86
14. Eisen, M., Spellman, P., Brown, P., & Botstein, D. J. (1998). Cluster analysis and display of genome-wide expression patterns. *Proceedings of the National Academy of Sciences of the United States of America*, 95, 14863–14868
15. Saldanha, A. J. (2004). Java Treeview–extensible visualization of microarray data. *Bioinformatics*, 20, 3246–3248
16. Zhang, L., Dong, Y., Wang, W., Zhao, T., Huang, T., Khan, A., Wang, L., et al. (2020). Ethionine Suppresses Mitochondria Autophagy and Induces Apoptosis via Activation of Reactive Oxygen Species in Neural Tube Defects. *Frontiers in neurology*, 11, 242
17. Zhang, L., Li, D., Zhang, J., Yan, P., Liu, X., Wang, L., Khan, A., et al. (2020). Excessive apoptosis and ROS induced by ethionine affect neural cell viability and differentiation. *Acta biochimica et biophysica Sinica*, 52, 1156–1165
18. Wang, Y., Li, H., & Song, S. P. (2018). beta-Arrestin 1/2 Aggravates Podocyte Apoptosis of Diabetic Nephropathy via Wnt/beta-Catenin Pathway. *Medical science monitor: international medical journal of experimental and clinical research*, 24, 1724–1732
19. Li, J., Xie, Q., Gao, J., Wang, F., Bao, Y., Wu, L. … Xie, J. (2021). Aberrant Gcm1 expression mediates Wnt/β-catenin pathway activation in folate deficiency involved in neural tube defects. *Cell death disease*, 12, 234
20. Blom, H., Shaw, G., den Heijer, M., & Finnell, R. (2006). Neural tube defects and folate: case far from closed. *Nature reviews. Neuroscience*, 7, 724–731
21. Berry, R., Li, Z., Erickson, J., Li, S., Moore, C., Wang, H., Mulinare, J., et al. (1999). Prevention of neural-tube defects with folic acid in China. China-U.S. Collaborative Project for Neural Tube Defect Prevention. *The New England journal of medicine*, 341, 1485–1490
22. Zhang, Q., Bai, B., Mei, X., Wan, C., Cao, H., Li, D., Wang, S., et al. (2018). Elevated H3K79 homocysteinylation causes abnormal gene expression during neural development and subsequent neural tube defects. *Nature communications*, 9,

3436

23. Luo, S., Zhang, X., Yu, M., Yan, H., Liu, H., Wilson, J., & Huang, G. Folic acid acts through DNA methyltransferases to induce the differentiation of neural stem cells into neurons. Cell biochemistry biophysics. 66:559–566
24. Bannister, A. J., & Kouzarides, T. (2005). Reversing histone methylation. *Nature*, 436, 1103–1106
25. Martin, C., & Zhang, Y. (2005). The diverse functions of histone lysine methylation. *Nature reviews Molecular cell biology*, 6, 838–849
26. Ge, K. (2012). Epigenetic regulation of adipogenesis by histone methylation. *Biochimica et biophysica acta*, 1819, 727–732
27. Zhang, Q., Xue, P., Li, H., Bao, Y., Wu, L., Chang, S., Niu, B., et al. (2013). Histone modification mapping in human brain reveals aberrant expression of histone H3 lysine 79 dimethylation in neural tube defects. *Nature communications*, 54, 404–413
28. Imbard, A., & Benoist, J. (2013). Blom HJljoer, health p. Neural tube defects, folic acid and methylation. *Birth Defects Res A Clin Mol Teratol*, 10, 4352–4389
29. Pogribny, I., Ross, S., Tryndyak, V., Pogribna, M., Poirier, L., & Karpinets, T. J. C. (2006). Histone H3 lysine 9 and H4 lysine 20 trimethylation and the expression of Suv4-20h2 and Suv-39h1 histone methyltransferases in hepatocarcinogenesis induced by methyl deficiency in rats. *Carcinogenesis*, 27, 1180–1186
30. Jackson, M., Krassowska, A., Gilbert, N., Chevassut, T., Forrester, L., Ansell, J., Ramsahoye, B. J. M., et al. (2004). Severe global DNA hypomethylation blocks differentiation and induces histone hyperacetylation in embryonic stem cells. *Molecular cellular biology*, 24, 8862–8871
31. Sahakyan, V., Pozzo, E., Duelen, R., Deprest, J., & Sampaolesi, M. J. (2017). Methotrexate and Valproic Acid Affect Early Neurogenesis of Human Amniotic Fluid Stem Cells from Myelomeningocele.Stem cells international, :6101609
32. Yu, J., Wang, L., Pei, P., Li, X., Wu, J., Qiu, Z., Zhang, J., et al. (2019). Reduced H3K27me3 leads to abnormal Hox gene expression in neural tube defects. *Epigenetics chromatin*, 12, 76
33. Nouri, P., Götz, S., Rauser, B., Irmler, M., Peng, C., Trümbach, D. … Dlugos, A. (2020). Dose-Dependent and Subset-Specific Regulation of Midbrain Dopaminergic Neuron Differentiation by LEF1-Mediated WNT1/b-Catenin Signaling. *Frontiers in cell developmental biology*, 8, 587778
34. Zhao, T., Gan, Q., Stokes, A., Lassiter, R. N., Wang, Y., Chan, J. … Zhou (2014). CJ. β-catenin regulates Pax3 and Cdx2 for caudal neural tube closure and elongation. *Development*, 141, 148–157
35. Yamaji, S., Droggiti, A., Lu, S., Martinez-Chantar, M., Warner, A., Varela-Rey, & MJEjocb (2011). S-Adenosylmethionine regulates connexins sub-types expressed by hepatocytes. *European journal of cell biology*, 90, 312–322
36. Li, T., Peng, H., Yang, H., Kurniawidjaja, S., Panthaki, P., Zheng, Y., Mato, J., et al. (2015). S-Adenosylmethionine and methylthioadenosine inhibit β-catenin signaling by multiple mechanisms in liver and colon cancer. *Molecular pharmacology*, 87, 77–86
37. Liu, Y., Lv, W., Yu, B., Ju, T., Yang, F., Jiang, M., Liu, Z., et al. (2013). S-adenosylmethionine-induced adipogenesis is accompanied by suppression of Wnt/β-catenin and Hedgehog signaling pathways. *Molecular cellular biochemistry*, 382, 59–73
38. Mansour, A., Gafni, O., Weinberger, L., Zviran, A., Ayyash, M., Rais, Y. … Amann-Zalcenstein, D. (2012). Maza, I. The H3K27 demethylase Utx regulates somatic and germ cell epigenetic reprogramming. *Nature*, 488, 409–413
39. Chen, X., Zhou, B., Yan, T., Wu, H., Feng, J., Chen, H., Gao, C., et al. (2018). Peroxynitrite enhances self-renewal, proliferation and neuronal differentiation of neural stem/progenitor cells through activating HIF-1α and Wnt/β-catenin signaling pathway. *Free radical biology medicine*, 117, 158–167

Figures

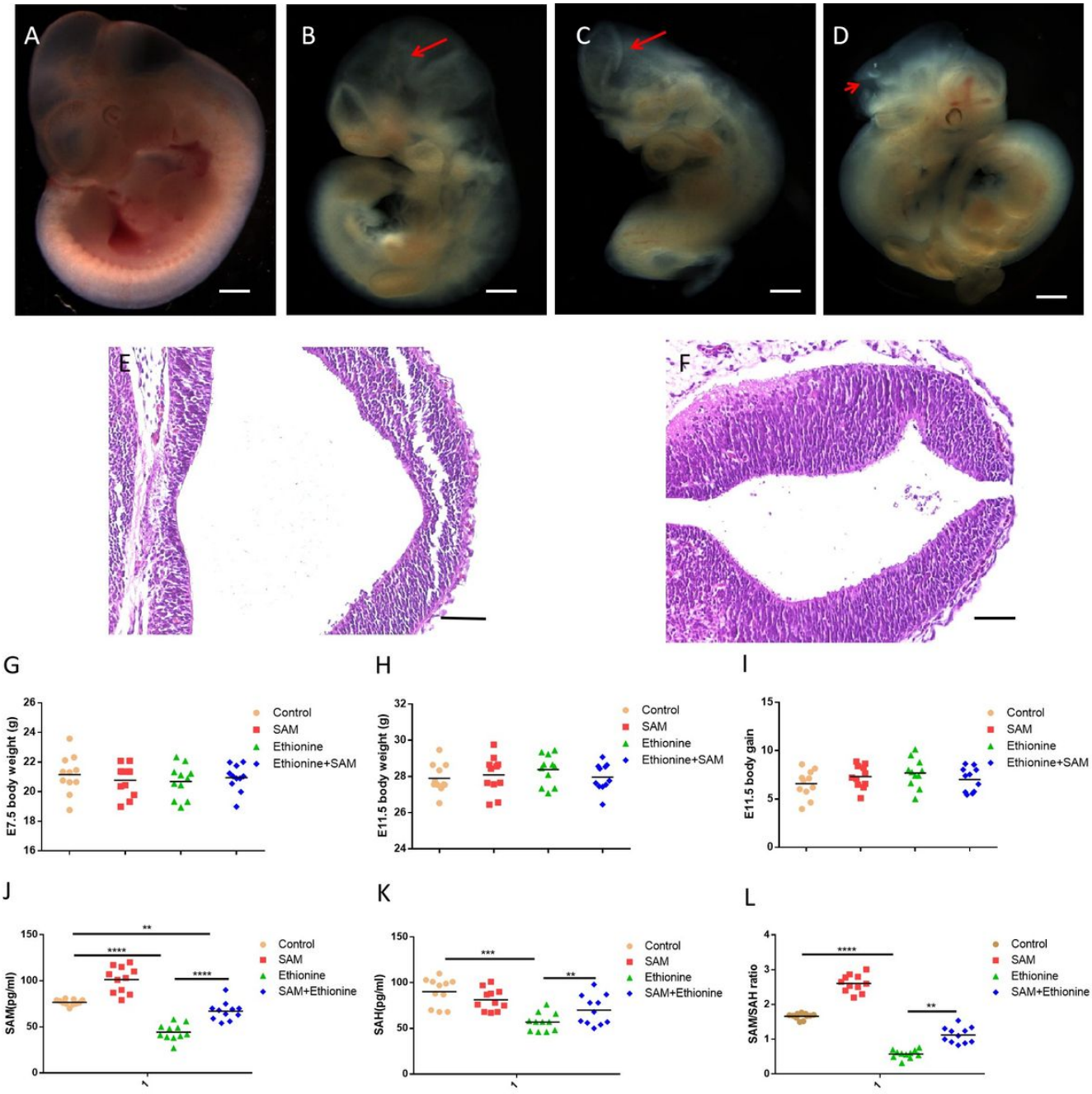

Figure 1

Ethionine induced neural tube defects by disrupting the methionine cycle. (A-D) Ethionine-induced anencephaly in C57BL/6 mouse embryos at E11.5. Scale bars, 500 μm. (E-F) H&E staining results of normal and NTDs embryonic neural tube in E11.5. Scale bars, 100 μm. (G) Quantitative detection of the body weight of C57 BL/6 pregnant mouse at E7.5 (n=11). (H) Quantitative detection of the body weight of C57 BL/6 pregnant mouse at E11.5 (n=11). (I) The weight difference between E11.5 and E7.5 of C57 BL/6 pregnant mouse (n=11). (J) The abundance of SAM was significantly lower in ethionine-induced mouse embryos than in nornmal embryos (**p < 0.01). However, treating with 2 mM SAM, the levels of SAM were increased significantly. (K) SAH was reduced, and the SAM/SAH ratio (L) was reduced in ethionine-induced mouse embryos compared with nornmal (**p < 0.01), which is significantly different from Control. Similarly, after giving 2 mM SAM compensation, the levels of SAH and SAM/SAH ratio were increased significantly (*p < 0.05). samples number for mouse embryos were 11 (n=11).

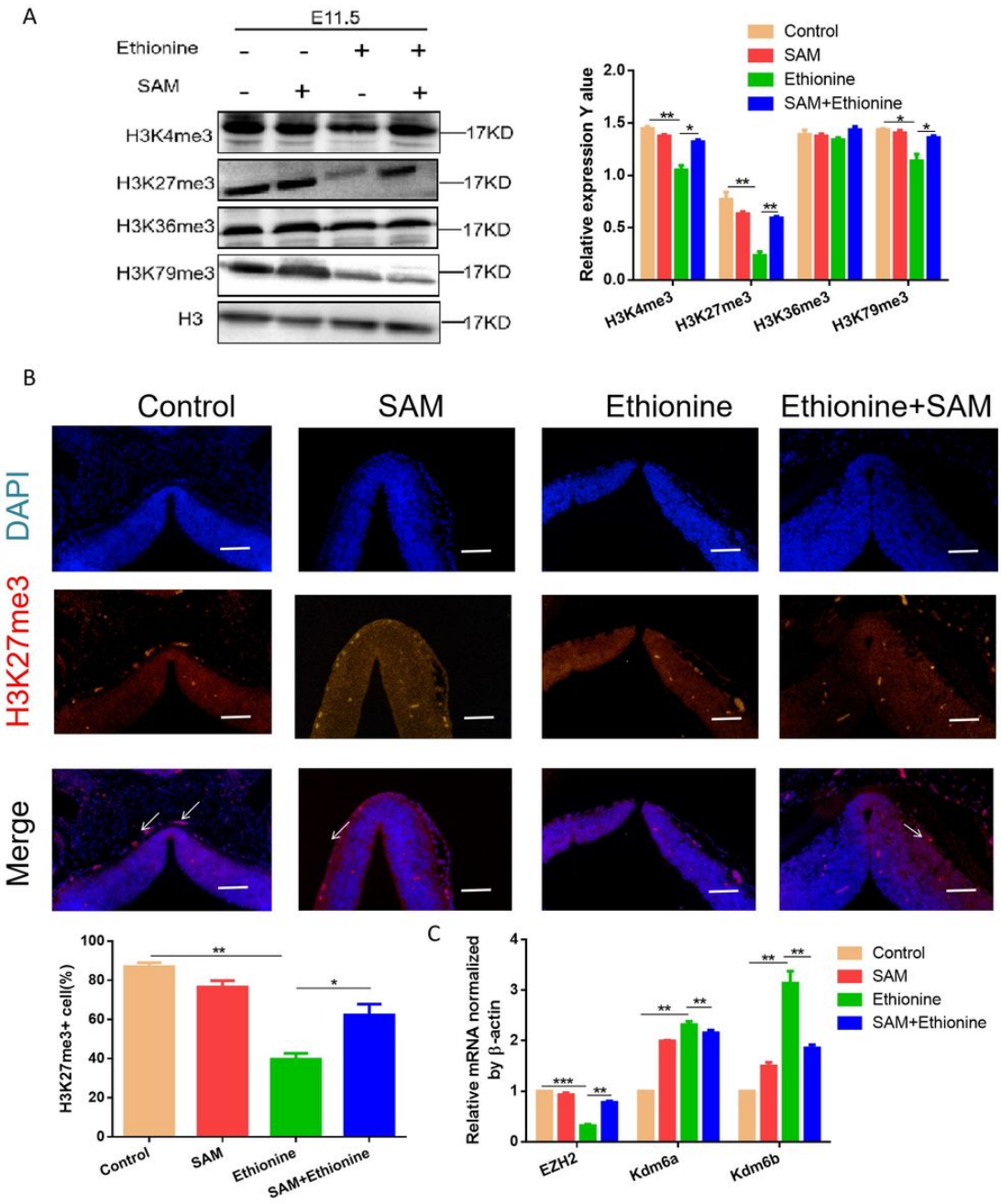

Figure 2

SAM enhanced the histone methylation levels of E11.5 embryonic brain tissue. (A) The results showed that the levels of H3K4me3, H3K27me3, H3K36me3 and H3K79me3 were decreased in E11.5, and the difference was statistically significant. The bar graph showed the quantification data (*p<0.05). (B) H3K27me3 (red signals) in the developing neuroepithelium of E11.5 embryos. Bar indicates 500 μm. (C) The mRNA levels of EZH2, Kdm6a and Kdm6b in E11.5 embryonic brain tissue treated with ethionine and SAM was measured by qRT-PCR. β-actin was used as a loading control. Data are shown a mean (n=3). *P<0.05.

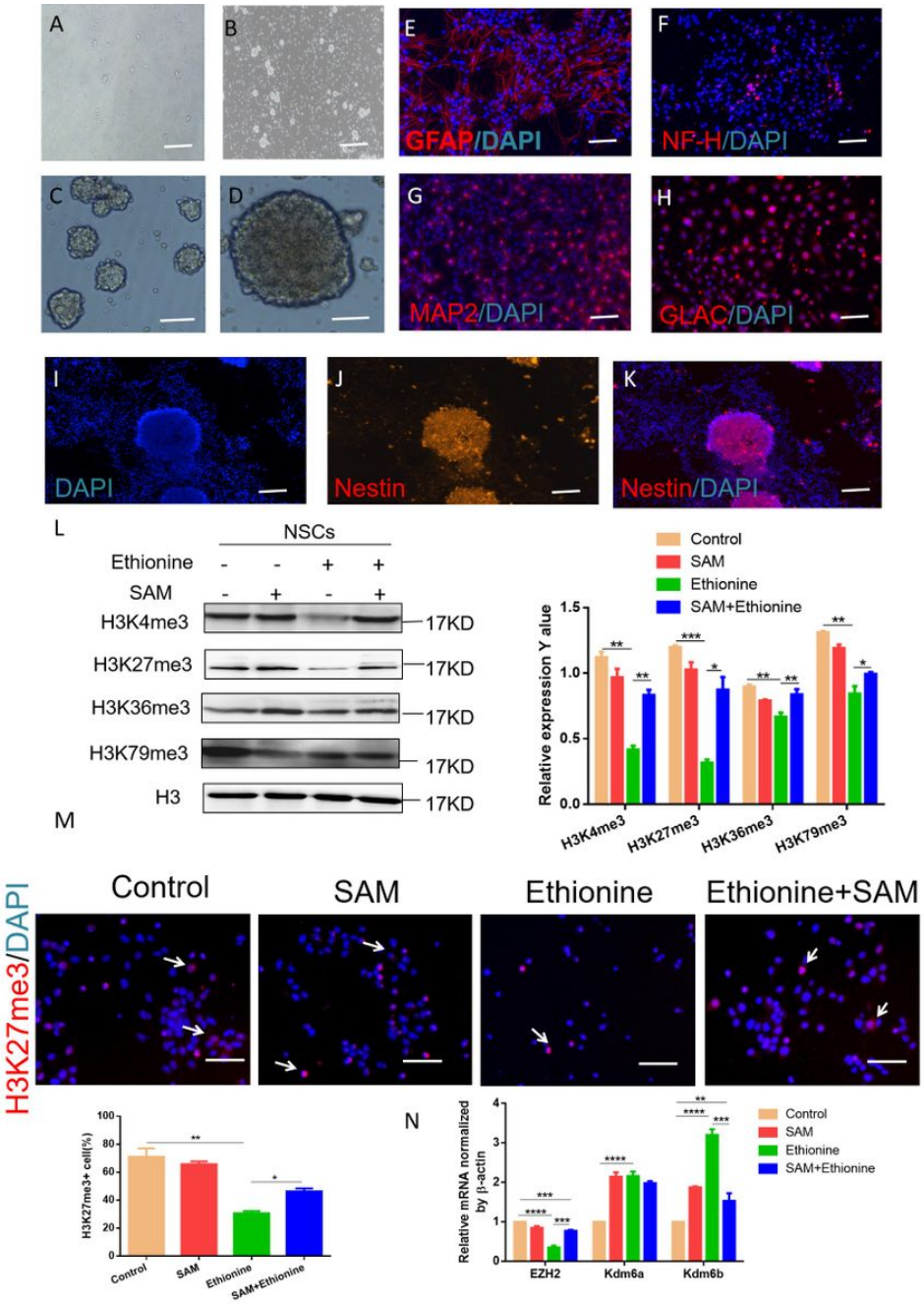

Figure 3

SAM Promoted the histone methylation level in NSCs. (A-D) NSCs derived from E13.5 embryos of wild-types mice were abnormal. Scale bar: 500 μm. (E-H) Identification of Map2-, GLAC-, NF-H-, and GFAP-positive NSCs by immunofluorescence. Scale bar in the fluorescence field: 500 μm. (I-K) Identification of Nestin- positive NSCs by immunofluorescence. Scale bar: 500 μm. (L) Administration of anti-methionine cycle metabolism inhibitor ethionine treatment in NSCs, compared with the control group, the levels of H3K4me3, H3K27me3 H3K36me3 and H3K79me3 were decreased in the experimental group, and the difference were statistically significant. *indicates significant difference compared with other groups in one-way ANOVA followed by Tukey tests. P<0.05. (M) H3K27me3 expression levels in the NSCs with 20mM eithionine and 2mM SAM for 24h by immunofluorescence. Scale bars, 100 μm. and the difference was statistically significant (*p<0.05). (N) The mRNA levels of EZH2, Kdm6a and Kdm6b in NSCs treated with ethionine and SAM was measured by qRT-PCR. β-actin was used as a loading control. Data are shown a mean (n=3). *P<0.05.

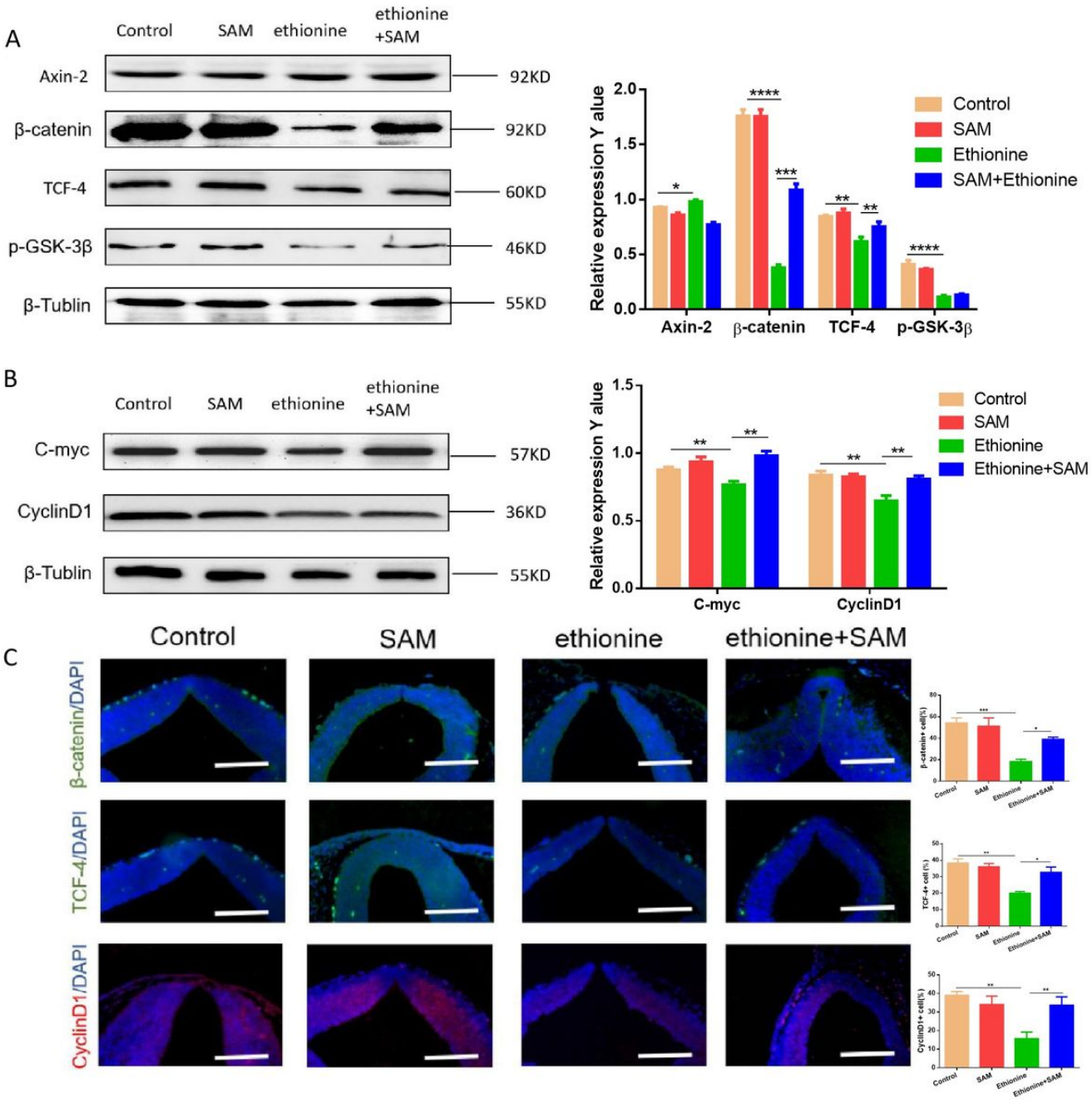

Figure 4

SAM stimulated Wnt/β-catenin signaling pathway in mouse embryos. The effect of ethionine induced on protein expression of Axin-2 (A), TCF-4 (A), β-catenin (A), p-GSK-3β (A), C-myc (B), CylinD1 (B) in the mouse embryos were treated with eithionine and SAM. Bar graphs for protein abundance were quantitative data from three independent experiments. *indicates significant difference compared with other groups in one-way ANOVA followed by Tukey tests. *P<0.05. (C) CyclinD1 (red signals), TCF-4 (green signals) and β-catenin (green signals) Low expression was observed in the neuroepithelia of E11.5 embryos. Bar indicates 100 μm. One-way ANOVA followed by LSD t-test were used for difference compared with other groups. *P < 0.05, **P < 0.01 and *** P < 0.001.

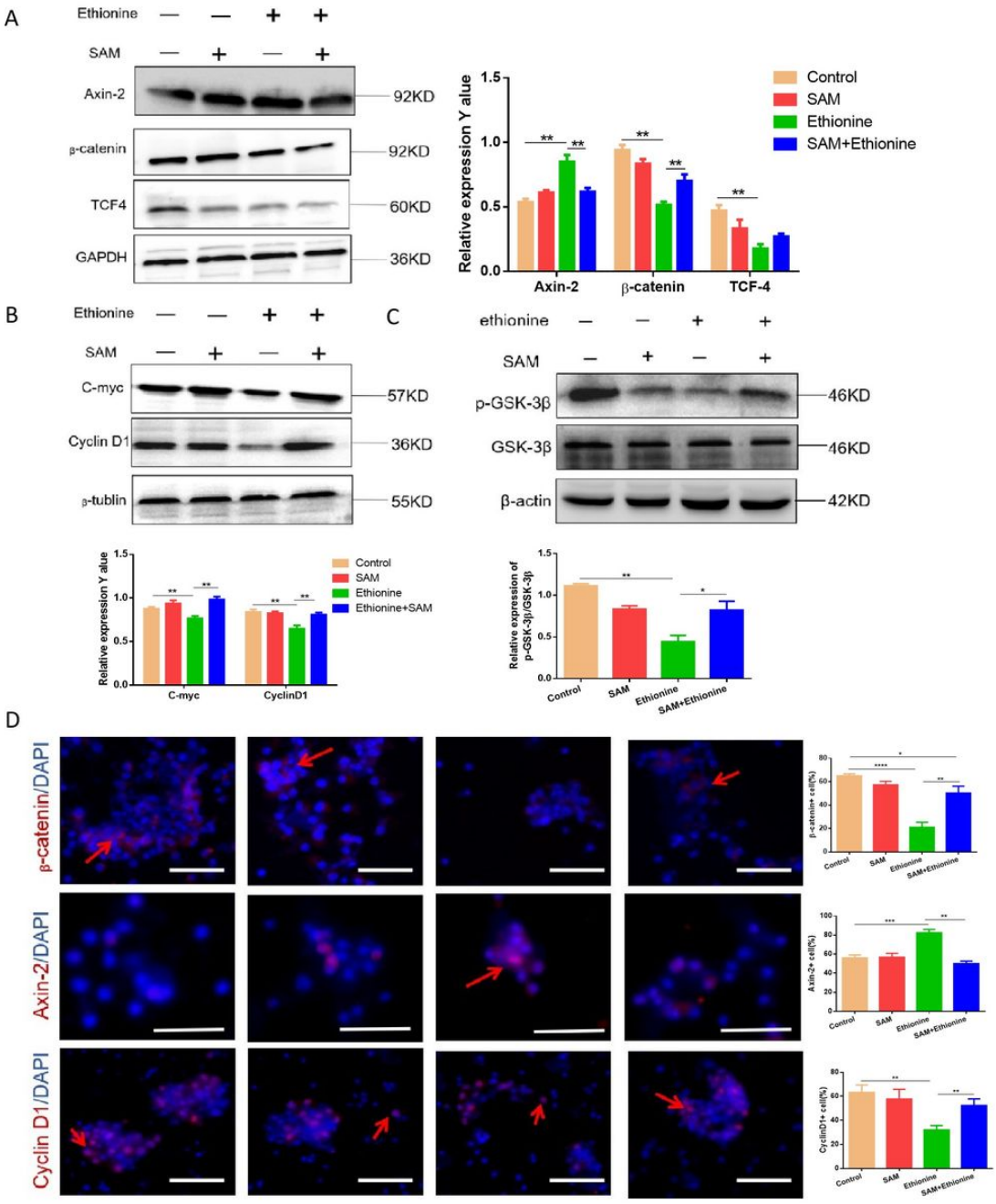

Figure 5

SAM accelerated Wnt/β-catenin signaling pathway in NSCs. (A) NSCs were treated with ethionine and SAM, Wnt/β-catenin signaling pathway related mark-of Axin-2, TCF4 and β-catenin protein level in control and experimental groups, (B) C-myc and CylinD1 protein levels in control and experiment groups and (C) p-GSK-3β protein levels in control and experiment groups were evaluated via Western blotting. For β-actin level was evaluated to confirm equal loading (n = 3). (D) Fluorescence microscopy analysis of β-catenin (red), CylinD1 (red), Axin-2 (red) staining in NSCs after treatment with ethionine and SAM for 24 h. Nuclei were also stained with DAPI, and representative single optical and merge images are shown. Scale bars: 100μm. Each experiment was carried out in triplicates. One-way ANOVA followed by LSD t-test were used for difference compared with other groups, *P < 0.05, **P < 0.01, ***P < 0.001, and ****P < 0.0001.

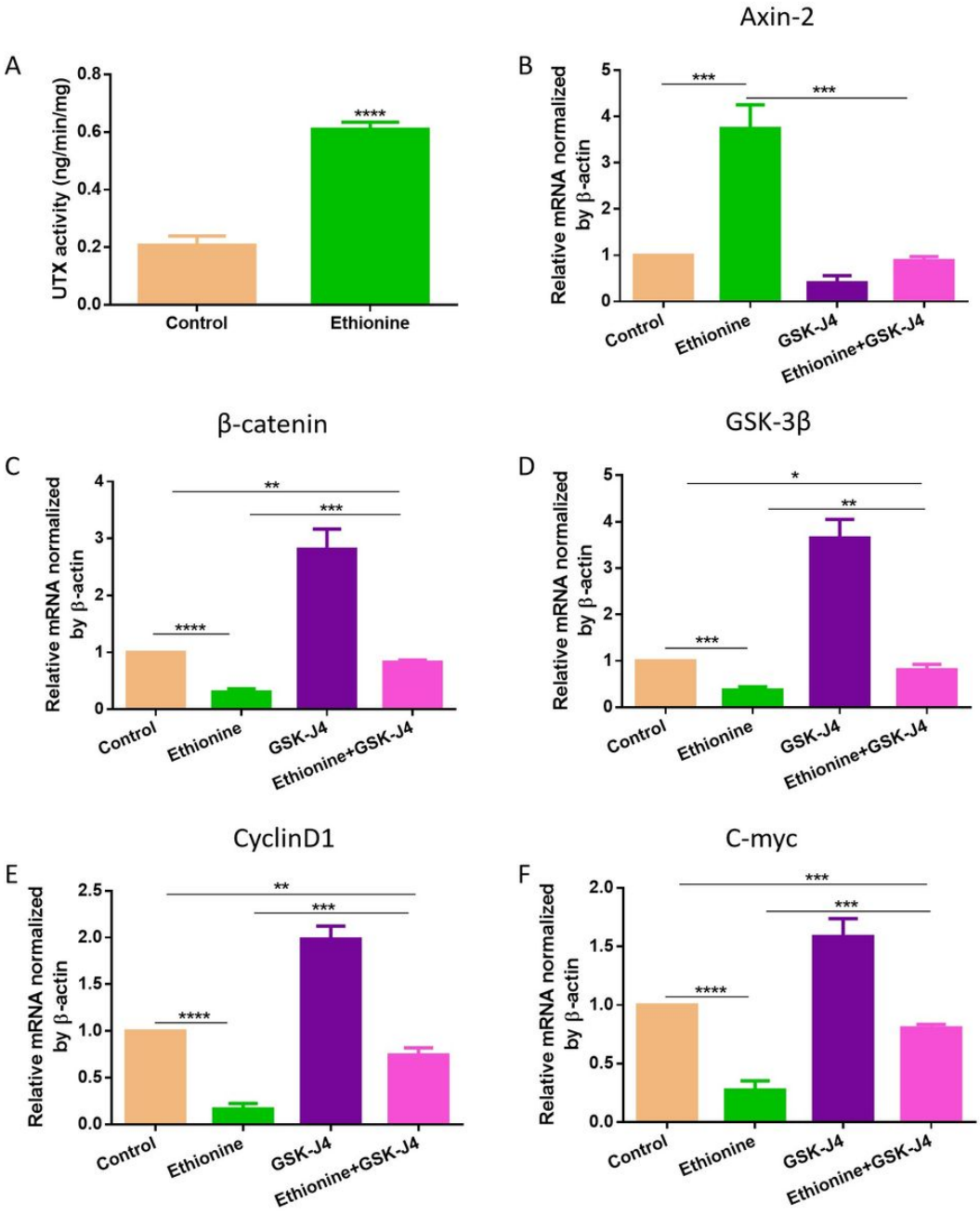

Figure 6

Reduced UTX activated Wnt/β-catenin signaling pathway. (A) UTX demethylase activity was detected in NSCs after ethionine treatment. Data are shown as the mean (n=3). ****P<0.0001. (B-F) The mRNA levels of β-catenin (C), Axin-2 (B), GSK-3β (D), CyclinD1 (E), and C-myc (F) in NSCs treated with ethionine and UTX inhibitor GSK-4J was measured by RT-qPCR. β-actin was used as a loading control. Data are shown as the mean (n=3). *P < 0.05, **P < 0.01, ***P < 0.001, and ****P < 0.0001.

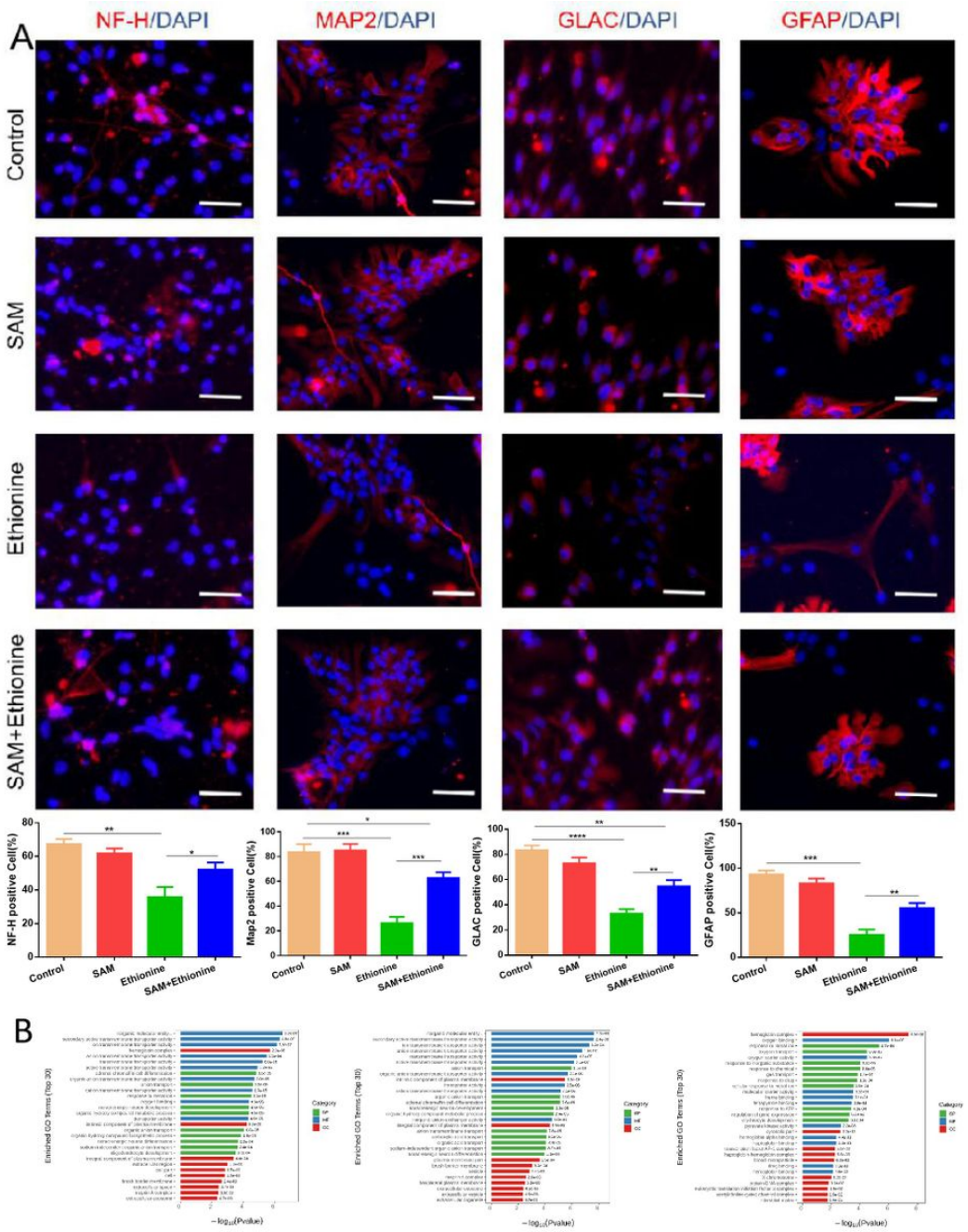

Figure 7

Ethionine inhibited NSCs differentiation. (A) At the level of neural stem cells, after the intervention with 20mM eithionine and 2mM SAM for 24h, the ability of GLAC, GFAP, MAP2, NF-H to differentiate was detected by Fluorescence microscopy analysis (P<0.001). Bar graph was the quantification data of density. *indicates significant difference compared with other groups in one-way ANOVA followed by Tukey tests. *P < 0.05, **P < 0.01, ***P < 0.001, and ****P < 0.0001. (B) GO functional classification of DEGs (corrected P value< 0.05). Top enriched GO terms of 10 cellular components, 10 molecular functions and 10 biological processes were shown.

Supplementary Files

This is a list of supplementary files associated with this preprint. Click to download.

- GraphicalAbstract.jpg